A RAPID PROTOTYPING DESIGN TOOL FOR PEAR HARVEST-AID PLATFORMS UTILIZING 3D FRUIT REACHABILITY AND KINEMATIC MODELING

Stavros Vougioukas[1], David Slaughter[1], Fadi Fathallah[1], Rachel Elkins[2], Chuck Ingels[3]

[1]Biological and Agricultural Engineering Department, University of California, Davis.
[2]University of California Cooperative Extension, Lake and Mendocino Counties.
[3]University of California Cooperative Extension, Sacramento County.

ABSTRACT

The design of any tree harvesting or harvest-aiding mechanized system should take into account the spatial distribution of fruits in the canopy. After all, reaching and picking fruits defines the function of such systems. However, registering fruit locations on trees has been a very time-consuming and expensive process. Therefore, in the past 60 years very few attempts at doing so have been reported in the literature. For this reason, a novel sensing system was developed that can record the locations of fruits on pear trees at a speed comparable to the fruit picking speed during commercial harvest. The system was used in the summer of 2012 to provide a large set of data for Bartlett and Bosc pears on trees of the standard 'open-vase' training system. The data were post-processed and fruit locations were computed for more than 15,000 pears. The collected data will be used as input to rapid-prototyping software that will be developed to assist in the design and evaluation of orchard automation machinery.

1. OBJECTIVES

The main objective of this project was to measure and record the positions of pear fruits in a large number of tree canopies along orchard rows. To accomplish this objective, three major goals were set: a) develop the necessary hardware and software infrastructure for data acquisition; b) perform field experiments during the harvesting season; c) develop algorithms and process the data to extract the position information and useful statistics.

2. PROCEDURES

A novel method was developed, which utilizes high-frequency ultra-wide band radio signals, and trilateration. More specifically, during manual harvesting, each fruit picker carried a mobile radio transmitter and receiver on his belt and wore gloves, with an antenna attached on each glove (Fig. 1). The antennas of both hands were connected to a radio transmitting and receiving unit (Fig. 2). A mobile trailer carried four radio

receiver-transmitter units (beacons) and corresponding antennas (Fig. 3); the distance of each beacon antenna from the antenna on each worker's hand was measured periodically. By combining the four distances of each antenna from the beacons, the three-dimensional coordinates of each glove were computed, with respect to the trailer. The trailer was equipped with a high-precision GPS (Fig. 4) that measured the geographical position of the trailer with an accuracy of less than one inch, and an inclinometer, i.e., an attitude sensor that measured roll, pitch and heading trailer angles. Using the data from these two sensors, the geo-referenced coordinates of the worker gloves with respect to the world frame (UTM) were computed. Finally, every time a worker picked a fruit, the event was registered manually by pushing a button on a wireless controller; the glove position at that time instant gave us the approximate position of the grasped pear. Next, details about the equipment and the computational procedures are given.

Fig. 1 Antenna in protective enclosure.

Fig. 2 Wearable transmitter - receiver unit.

Fig. 3 Trailer with four radio beacons on poles.

Fig. 4 GPS receiver and RTK base-link antenna.

2.1 Materials and Methods

Next, the equipment that was used for the data collection experiments will be described in detail with emphasis on its functional specifications. The mathematical procedure to compute the fruit locations from the range data and the trailer position and attitude data will also be described in detail.

2.1.1 Ranging System

The radio receiving and transmitting unit used in this research is the Time Domain's PulsON 400 Ranging and Communications Module (P400 RCM). The P400 RCM is an Ultra Wideband (UWB) radio transceiver that accurately and reliably measures the distance between two P400 RCMs (Fig. 5) and provides these measurements at a high update rate. It also provides the following functions:

1. It supports two different range measurement techniques (Two-Way Time-of-Flight and Coarse Range Estimation).
2. It communicates data between two or more RCMs.

The units operate in the band of 3.1GHz to 5.3 GHz with a center frequency at 4.3 GHz. In a static scenario (units not moving) with a clear Line of Sight (LOS), the specifications for the range measurement precision (standard deviation) is 2.3 cm (0.9''), and for accuracy (bias) is 2.1 cm (0.83''). The system was used with a PII=7, which means that the maximum range was 125 m (410 ft), and each measurement required 20 ms to be completed.

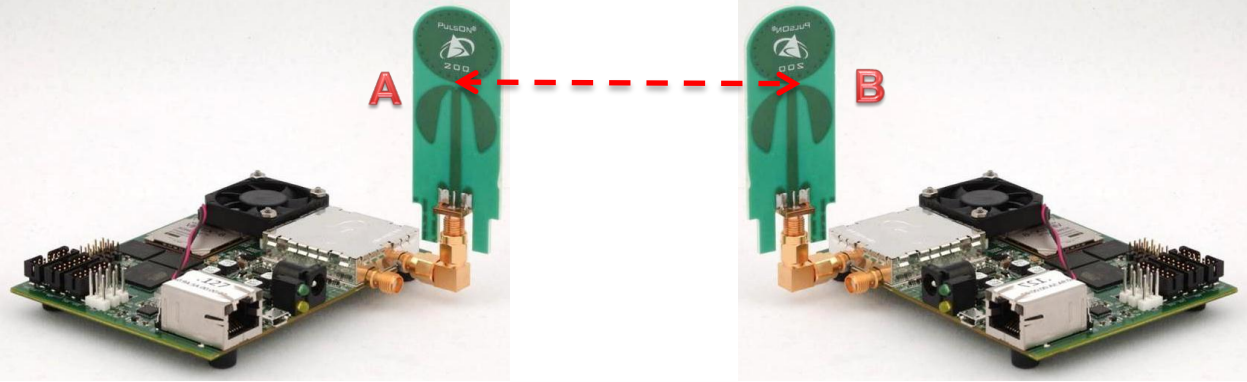

Fig. 5 Unit A measures distance (red dotted line) between center points of antennas A and B.

2.1.2 GPS System

The Trimble AgGPS 542 GNSS/RTK 900Mhz Rover GPS System was used to collect real-time, high-accuracy field geo-referenced point location data. Since data were collected while the trailer was static, the data acquisition rate was kept low, at 1Hz. The Ag542 Rover receives GPS corrections from the Ag 542 Mobile Base Station Kit. Both the Ag542 Base & Rover feature Integrated 900Mhz Radios and 72 Channels capable of receiving GPS (L1/L2), GLONASS, & GPS Modernization (L2C) satellite signals, which improves accuracy and performance even in tough satellite environments.

2.1.3 Attitude and Heading Sensor

A wireless attitude and heading sensor by Yost Engineering was used to measure the trailer's roll, pitch and heading angles (Fig. 6). This is a high-precision, high-reliability system with a 2.4GHz DSSS communication interface and a rechargeable lithium-polymer battery. It uses triaxial gyroscope, accelerometer, and compass sensors in conjunction with advanced processing and on-board quaternion-based Kalman filtering algorithms to determine orientation relative to an absolute reference in real-time. It has $\pm 1^{o}$ orientation accuracy for dynamic conditions, and repeatability < 0.008^{o}. It allows access to raw sensor data, normalized sensor data, and filtered absolute and relative orientation outputs in multiple formats including: quaternion, Euler angles (pitch/roll/yaw), rotation matrix, axis angle, two-vector (forward/up). The sensor uses a left-handed system as shown below (Fig. 7).

Fig. 6 Wireless attitude and heading sensors.

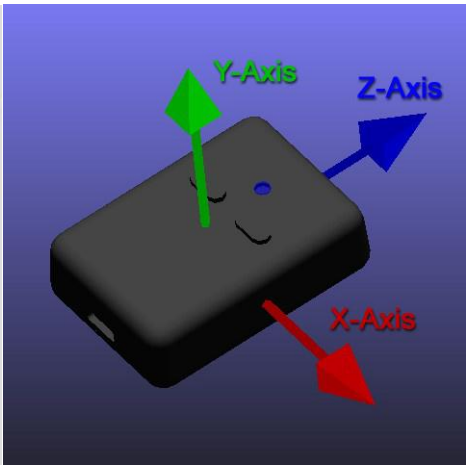

Fig. 7 Sensor reference frame.

The computed order of rotation is XZY. Therefore, the total Euler rotation matrix, *R* is composed of three rotation matrices, multiplied as $R = R_y R_z R_x$. The three angles are reported by each sensor as *ψ*, *θ*, *φ*, where pitch (*ψ*) is rotation about the X axis (looking towards X: 0, clockwise is positive), heading (*θ*) is about the Y axis (looking towards Y: 0, clockwise is positive), and roll (*φ*) is about the Z axis (looking towards Z: 0, clockwise is positive).

2.1.4 Geo-referencing and Trilateration

First the following reference frames are defined: instantaneous trailer frame (*TF*); world frame (*WF*); instantaneous rover GPS frame (*GPSF*); instantaneous attitude sensor frame (*AF*); initial attitude sensor frame (*YTF*); trailer frame at initial position (*ITF*).

Let us also define the positions of all sensors on the trailer, expressed with respect to the trailer frame, in homogeneous coordinate vectors: position of the receive-transmit point on each RCM beacon antenna: ${}^{TF}\mathbf{b}_i = [x_i \; y_i \; z_i \; 1]^T$, *i*=1,2,3,4; position of the GPS receiver origin: ${}^{TF}\mathbf{p}_{GPSF} = [\Delta x_{gps} \; \Delta y_{gps} \; \Delta z_{gps} \; 1]^T$; origin of attitude sensor: ${}^{TF}\mathbf{p}_{YF} = [\Delta x_{yei} \; \Delta y_{yei} \; \Delta z_{yei} \; 1]^T$. All these positions were measured manually after installation on the trailer. All GPS positions are absolute geo-referenced coordinates with a Universal Transverse Mercator (UTM) projection.

Let also the position of the *i*th RCM beacon antenna expressed in the world frame be ${}^{WF}\mathbf{b}_i = \left[bx_i \; by_i \; bz_i \; 1\right]^T$.

Furthermore, the position of origin of the trailer frame expressed in the trailer GPS frame is ${}^{GPSF}\mathbf{p}_{TF} = [-\Delta x_{gps} \; -\Delta y_{gps} \; -\Delta z_{gps} \; 1]^T$. Let us also define the matrix *I*:

$$I = \begin{pmatrix} 1 & 0 & 0 \\ 0 & 1 & 0 \\ 0 & 0 & 1 \\ 0 & 0 & 0 \end{pmatrix} \quad (1)$$

Then, the homogeneous (4 x 4) coordinate transformation matrix of *GPSF* with respect to *TF* is ${}^{TF}H_{GPSF} = \begin{bmatrix} I & {}^{TF}\mathbf{p}_{GPSF} \end{bmatrix}$, and the transformation matrix of frame *TF* with respect to *GPSF* is ${}^{GPSF}H_{TF} = {}^{TF}H_{GPSF}^{-1} = \begin{bmatrix} I & {}^{GPSF}\mathbf{p}_{TF} \end{bmatrix}$. The instantaneous sensor measurements are given next: the position of the trailer GPS is ${}^{WF}\mathbf{p}_{GPSF} = [x_{gps} \; y_{gps} \; z_{gps} \; 1]^T$; the rotation of the attitude sensor with respect to the initial attitude sensor frame (*YTF*) is:

$${}^{YTF}R_{TF} = \begin{bmatrix} c\theta c\varphi & s\psi s\theta - c\psi c\theta s\varphi & c\psi s\theta + c\theta s\psi s\varphi \\ s\varphi & c\psi c\varphi & -c\varphi s\psi \\ -c\varphi s\theta & c\theta s\psi + c\psi s\theta s\varphi & c\psi c\theta - s\psi s\theta s\varphi \end{bmatrix} \quad (2)$$

Since the GPS and attitude sensors are rigidly attached on the trailer, the following transformations are equal, i.e., ${}^{YTF}R_{AF} = {}^{YTF}R_{TF} = {}^{YTF}R_{GPSF}$.
At each time instant, the rotation of the trailer with respect to the world frame can be computed as:

$${}^{WF}R_{TF} = {}^{WF}R_{ITF} \; {}^{ITF}R_{YTF} \; {}^{YTF}R_{AF} \quad (3)$$

The position of trailer frame expressed in the world frame as:

$${}^{WF}\mathbf{p}_{TF} = {}^{WF}H_{GPSF} \; {}^{GPSF}\mathbf{p}_{TF} = \begin{bmatrix} {}^{WF}R_{TF} & {}^{WF}\mathbf{p}_{GPSF} \\ 0 \; 0 \; 0 & \end{bmatrix} {}^{GPSF}\mathbf{p}_{TF} \quad (4)$$

At each time instant, the position of each trailer RCM ranging antenna expressed in the world frame can be computed as:

$${}^{WF}\mathbf{b}_i = {}^{WF}H_{TF} \; {}^{TF}\mathbf{b}_i = \begin{bmatrix} {}^{WF}R_{TF} & {}^{WF}\mathbf{p}_{TF} \\ 0 \; 0 \; 0 & \end{bmatrix} {}^{TF}\mathbf{b}_i \quad (5)$$

Let r_{ij} and $\hat{r}_{ij}$ be the true and measured distances between the ith RCM trailer beacon and the *j*th glove antenna respectively. Given the error ε_{ij} in each measurement, the following equation holds:

$$\hat{r}_{ij} = r_{ij} + \varepsilon_{ij} \quad (6)$$

The measured distance $\hat{r}_{ij}$ as a function of the unknown picker-glove antenna coordinates is given by:

$$\hat{r}_{ij} = \left((x_j - bx_i)^2 + (y_j - by_i)^2 + (z_j - bz_i)^2 \right)^{1/2} \quad (7)$$

Also, let the unknown positions of the *j*th antenna on the worker gloves expressed in the world frame be ${}^{WF}\mathbf{p}_j = [x_j^* \; y_j^* \; z_j^* \; 1]^T$. The coordinates can be computed by minimizing the total squared error:

$$(x_j^*, y_j^*, z_j^*) = \underset{x_j, y_j, z_j}{\arg\min} \sum_{i=1}^{4} \left(\hat{r}_{ij}^2 - \left((x_j - bx_i)^2 + (y_j - by_i)^2 + (z_j - bz_i)^2 \right) \right) \quad (8)$$

Each time a fruit is grasped by a worker, the timestamp of the "fruit-grasp" event is recorded along with the worker id, whether it is left or right hand, and which tree the fruit is picked from. The approximate coordinates of all picked fruits are computed by solving the above equation for all such events.

3. RESULTS

Fruit location data were gathered from the following sites:

DATE: 8/14/2012 WHAT: Pear trees, standard open-vase AGE: ~32 yrs TREE HEIGHT: 14-15 ft VARIETY: Bosc WHERE: Joe Green Ranch LAT. N 3819.93896114 LONG. W 12132.92408032	DATE: 8/20/2012 WHAT: Pear trees, standard open-vase AGE: ~ 32 yrs TREE HEIGHT: ~ 16 ft VARIETY: Red Bartlett WHERE: Johnson Family Ranch, Ukiah LAT. N 39 08 27.98288 LONG. W 123 11 28.90587
DATE: 8/21/2012 WHAT: Pear trees, standard open-vase AGE: Old trees ~50 yrs, Interplants ~15 yrs TREE HEIGHT: 13-14 ft VARIETY: Yellow Bartlett WHERE: Ruddick Ranch LAT. N 39 07 04.54903 LONG. W 123 10 30.87676	DATE: 8/22/2012 WHAT: Pear trees, standard open-vase AGE: Old trees ~42 yrs, Interplants ~37 yrs TREE HEIGHT: 14-15 ft VARIETY: Yellow Bartlett WHERE: Buss Ranch LAT. N 38 59 08.49753 LONG. W 122 50 05.49697

Data were also collected at the Malcolm McCormack Ranch in Courtland from a hedgerow-trained orchard. Unfortunately, due to technical and human errors those data are unusable. Also, half of the data from the Johnson Family Ranch were not usable because of a GPS malfunction that became obvious during the post-processing of the data.

3.1 Joe Green Ranch

Results from the field experiment at Joe Green Ranch (8/14/12) are given next. Data were collected from fifteen trees along a row shown in Fig. 8.

Fig. 8 Data collected at Joe Green Ranch (8/14/12) from fifteen pear trees inside the yellow rectangle.

A map of the fruit locations in 3D is shown in Fig. 9.

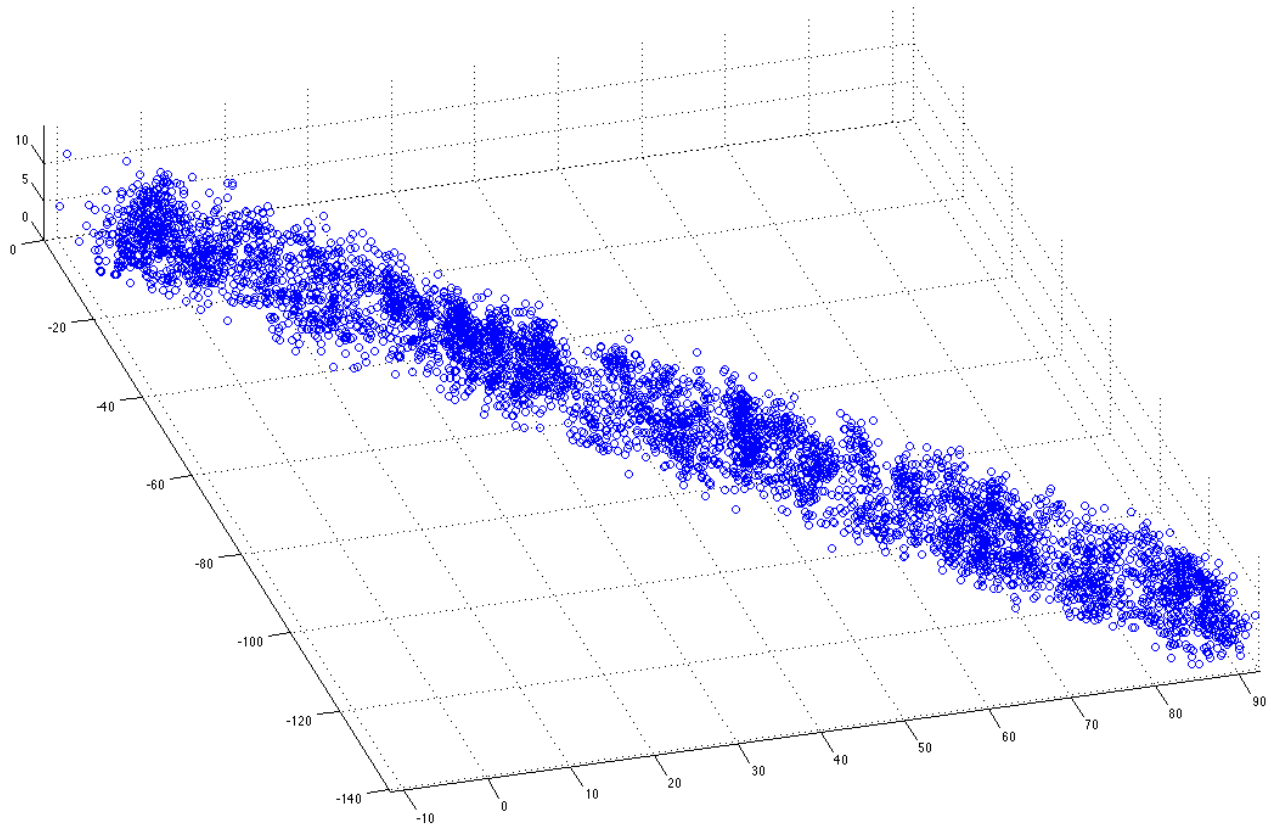

Fig. 9 Fruit locations in the canopies of fifteen trees in a row.

The yield of each tree can be seen in Fig. 10; an average of 516 fruits were collected per tree, with a standard deviation, σ = 92.6 fruits.

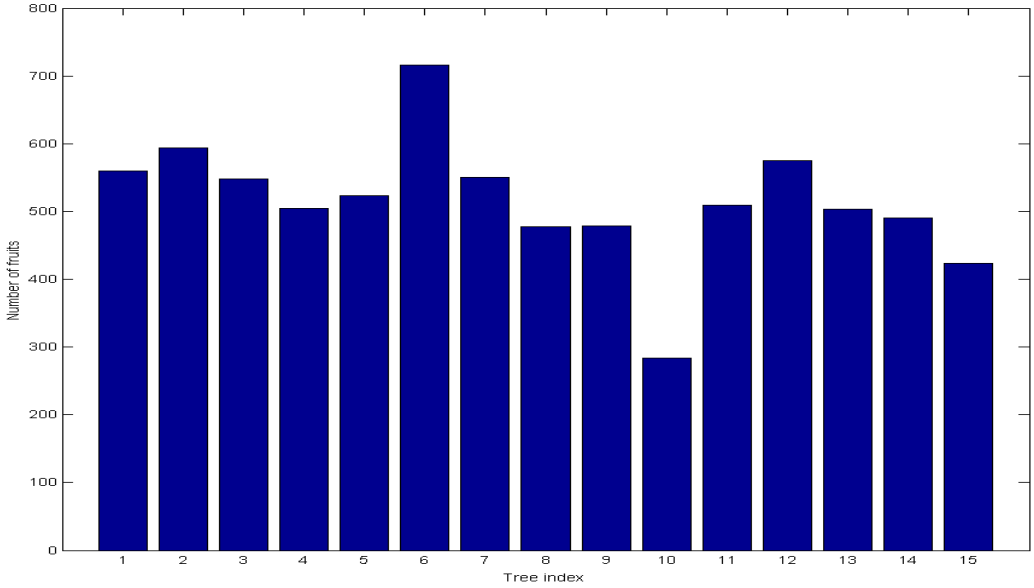

Fig. 10 Number of fruits (yield) per tree.

The height distribution of the pears in a row is very important for mechanization because it sets the specifications for the lifting system of any harvesting equipment. The normalized histogram for the fifteen trees in the row is given in Fig. 11

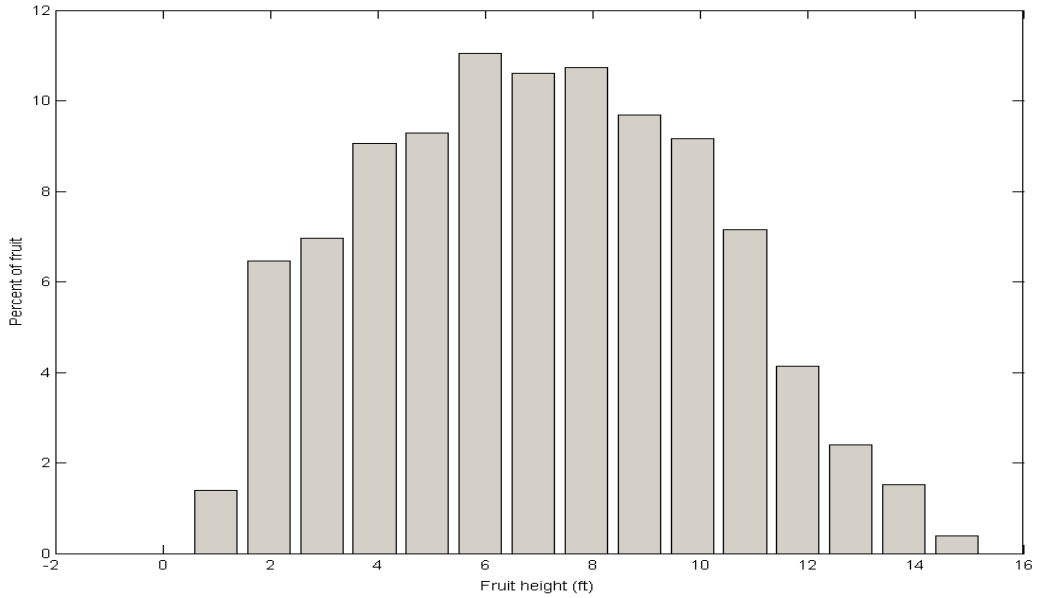

Fig. 11 Fruit height normalized histogram.

The corresponding cumulative height histogram is given in Fig. 12. It can be seen that these 32-year-old trees bear fruit from near the ground to their tops. In this orchard, about 55% of the fruit is above 6ft, i.e., the average picker on the ground cannot reach it.

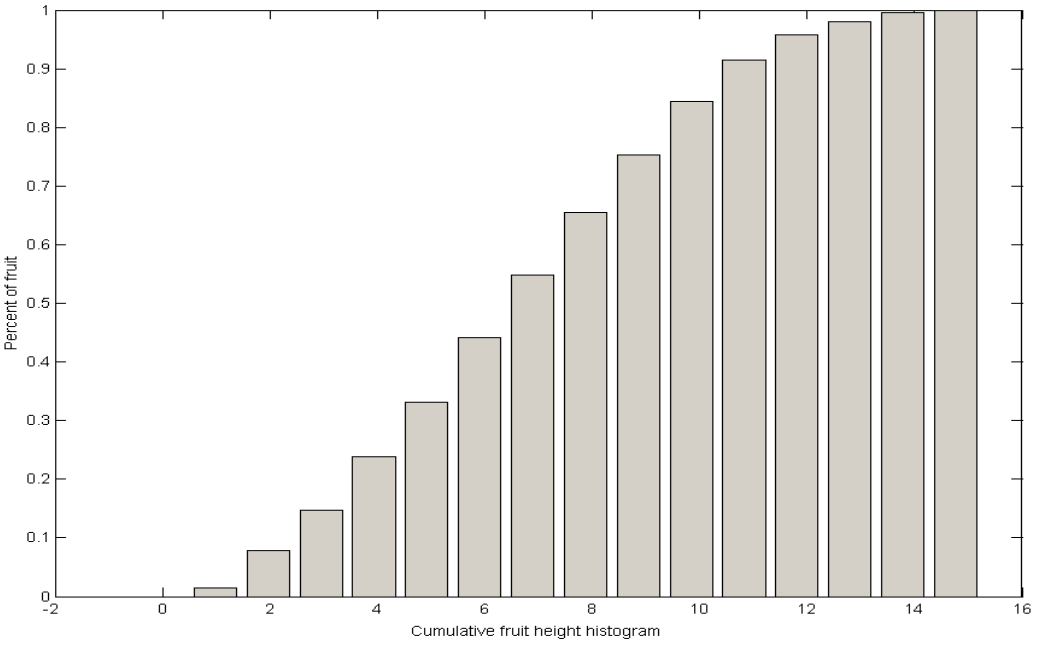

Fig. 12 Cumulative fruit height histogram.

Let us define for each fruit, its smallest distance, *d*, from the vertical planes in the middle of the rows to the right and left of the tree is defined. The normalized histogram of this distance is an approximation of the probability density function, i.e., the probability that a fruit is at a certain distance from the row centers. The standard deviation, σ, of this distribution can be used as a *metric* that expresses the uniformity of *fruit reachability* from a worker or machine moving along a row. The normalized histogram of this distance is shown in Fig. 13. This is an approximation to the probability density function of the distance variable. The mean value of this distance is E(*d*) = 5.88 ft, and the standard deviation, σ = 1.45 ft.

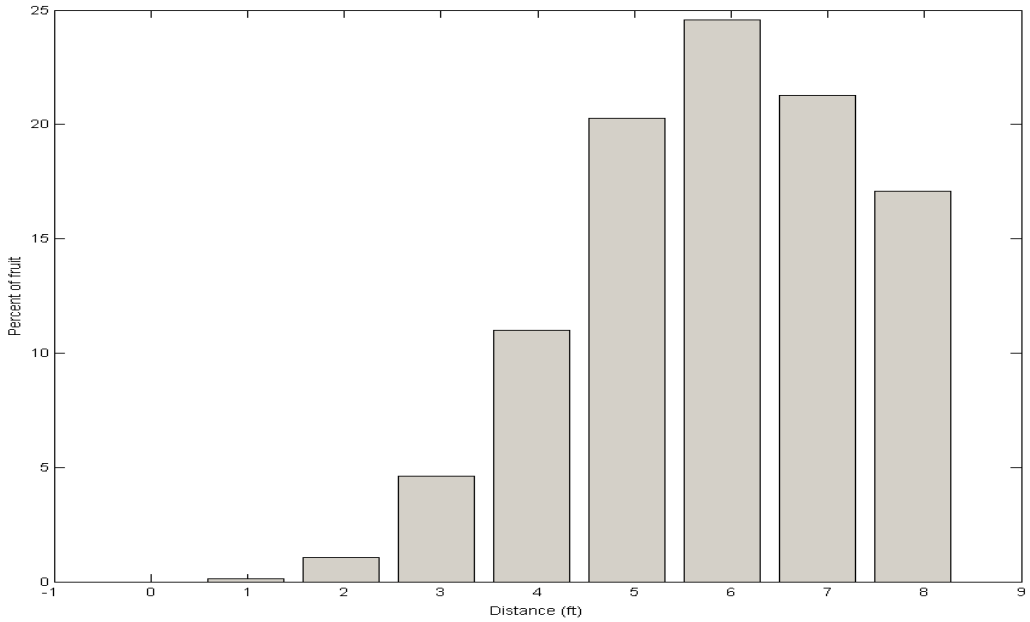

Fig. 13 Normalized histogram of fruit horizontal minimum distance from the left and right row centers.

The closest to zero the standard deviation is, the easier it is to reach fruit from the row without moving towards the tree or in the space between trees. Trees trained in hedgerows are expected to have a smaller standard deviation than standard open-vase trees.

3.2 Ruddick Ranch

Results from the field experiment at Ruddick Ranch (8/21/12) are given next.

Fig. 14 Data collected at Ruddick Ranch (8/21/12) from fifteen pear trees inside the yellow rectangle.

Data were collected from fifteen trees along a row shown in Fig. 14. A map of the fruit locations in 3D is shown in Fig. 15.

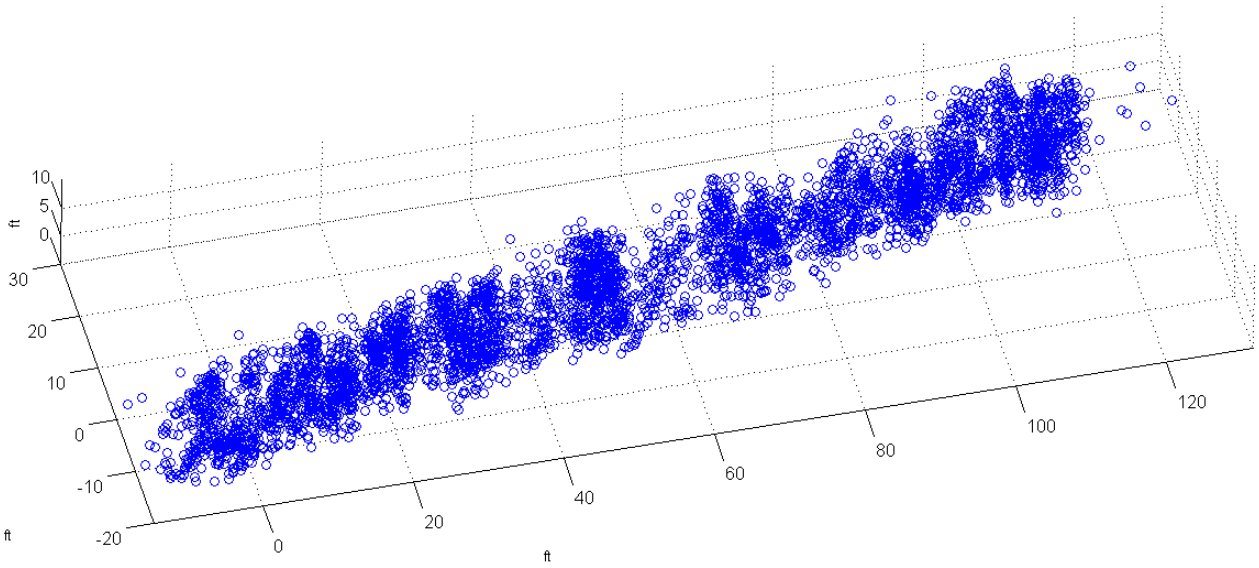

Fig. 15 Fruit locations in the canopies of fifteen trees in a row.

The yield of each tree can be seen in Fig. 16. The row contained old large trees and young small trees inter-planted; the difference in yield is clearly shown in the figure; however large yield variation exists also among the old trees.

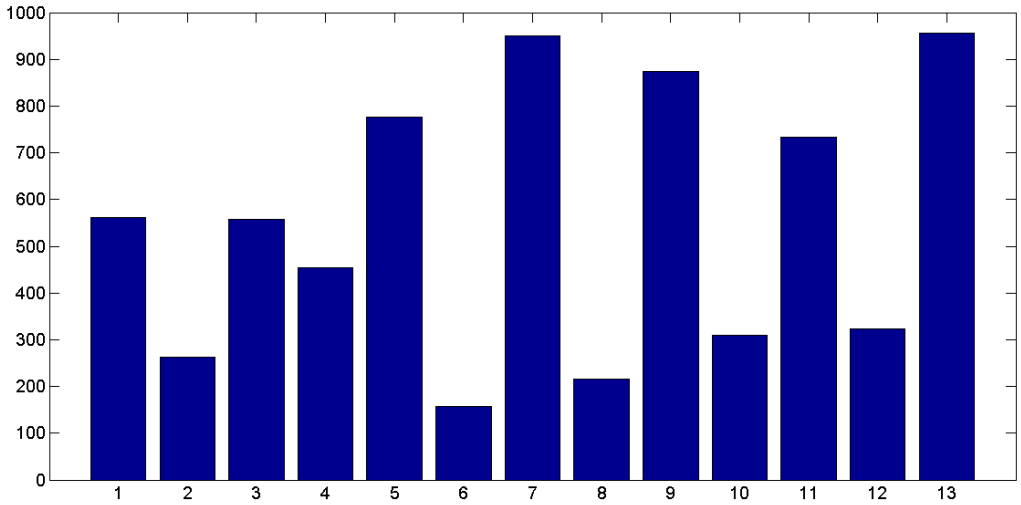

Fig. 16 Number of fruits (yield) per tree.

The height distribution of the pears for the fifteen trees in the row is shown in the normalized histogram in Fig. 17.

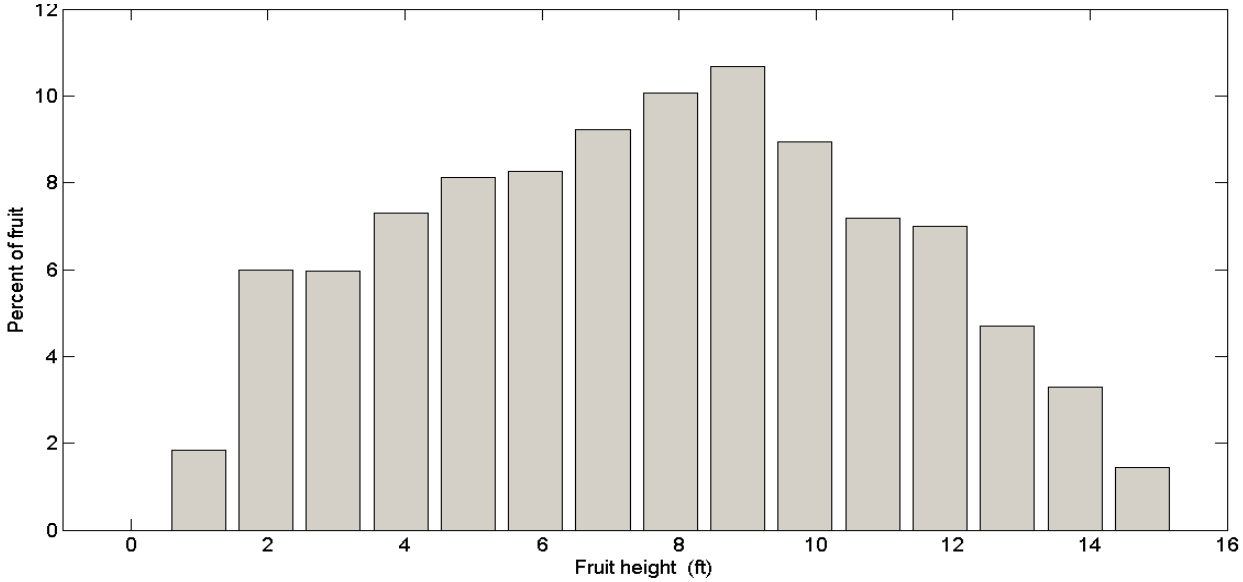

Fig. 17 Fruit height normalized histogram.

The corresponding cumulative height histogram is given in Fig. 18. It can be seen that these old trees bear fruit from near the ground to their tops. It is clear that 65% of the fruit is above 6ft, i.e., the average picker on the ground cannot reach it.

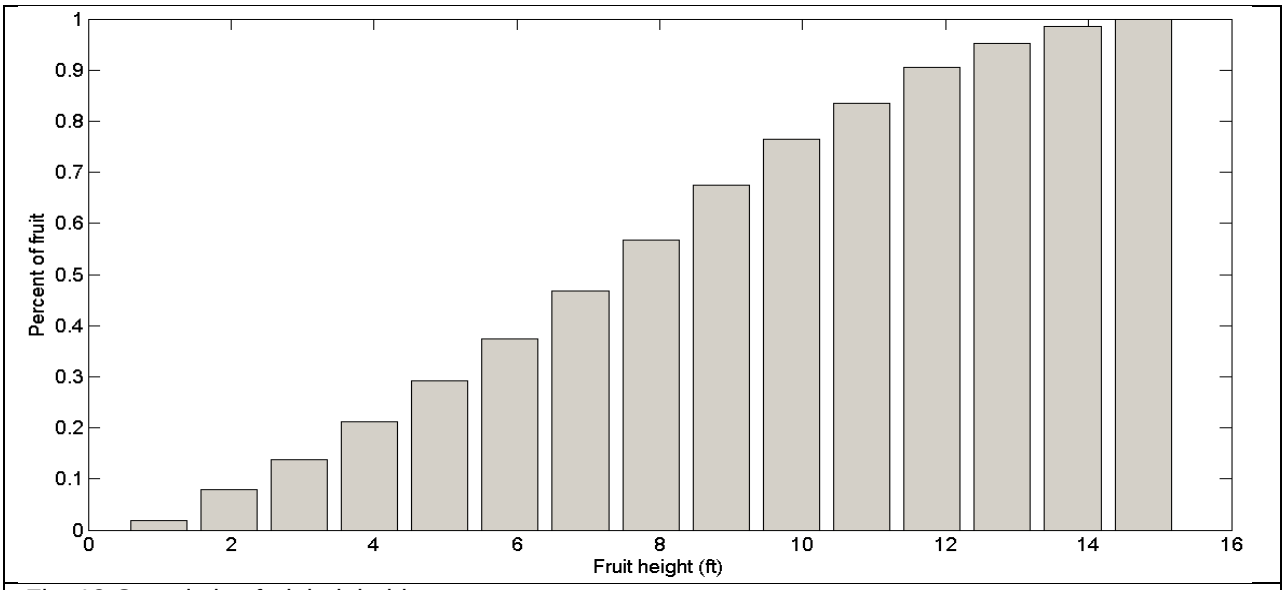

Fig. 18 Cumulative fruit height histogram.

The normalized histogram of the fruit distances from the row-centers is shown in Fig. 19. The mean value of this distance is E(d) = 6.74 ft, and the standard deviation, σ = 1.88 ft. This standard deviation is larger than the one measured at Joe Green ranch; in fact, based on visual inspection it can be said that the tree canopies at this part of the orchard were not as well pruned as in other parts of the same ranch or in the other orchards we visited.

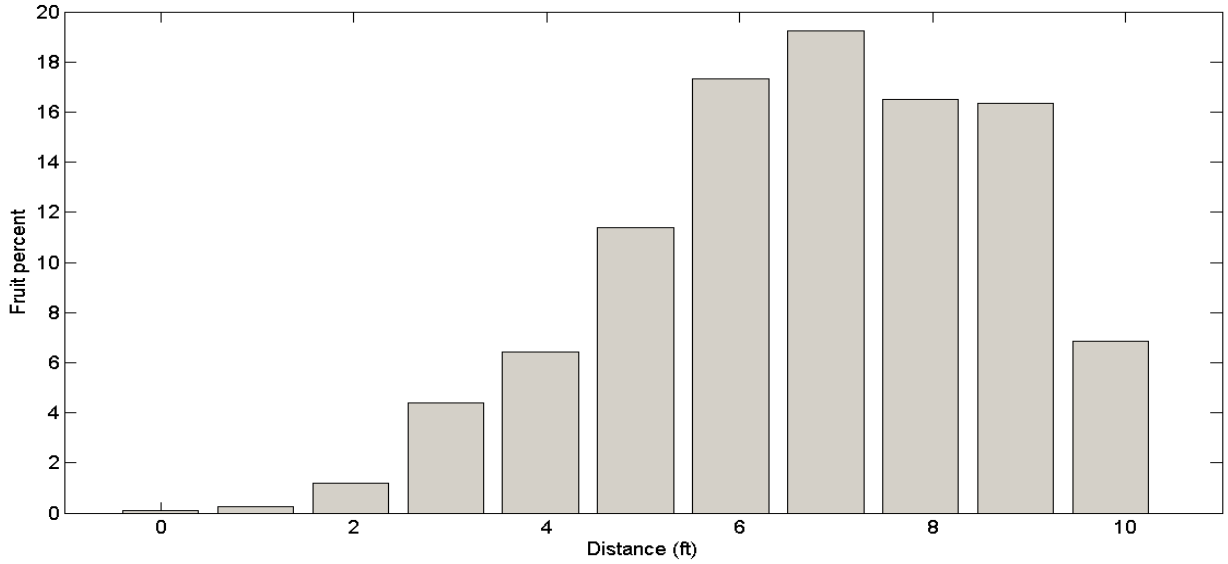

Fig. 19 Normalized histogram of fruit horizontal minimum distance from the left and right row centers.

3.3. Buss Ranch

Next, data from Buss Ranch (8/22/12) are given.

Fig. 20 Data collected at Buss Ranch (8/22/12) from fifteen pear trees inside the yellow rectangle.

The yield of each tree can be seen in Fig. 21. Again, the row contained inter-planting of old large trees and young small trees; the difference in yield is clearly shown in the figure; however large yield variation exists also among the old trees.

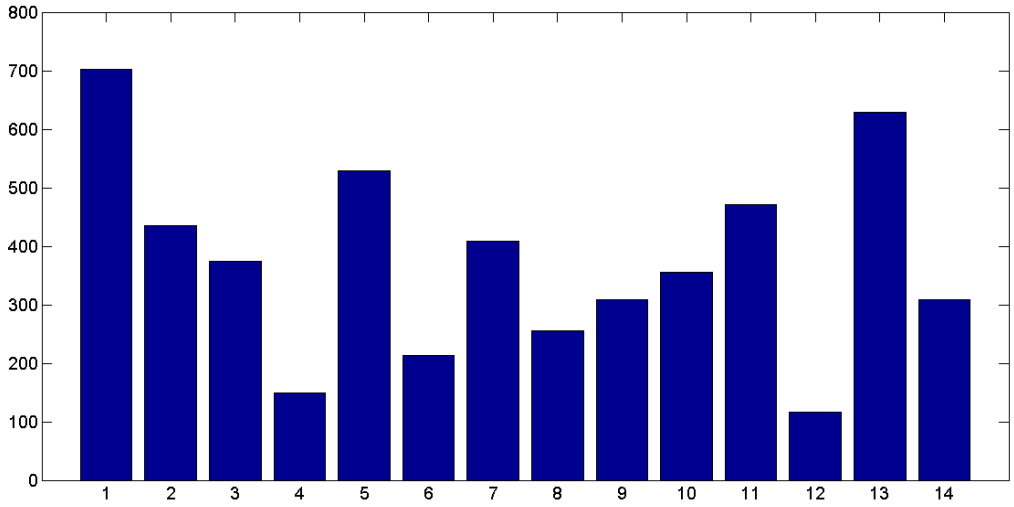

Fig. 21 Number of fruits (yield) per tree.

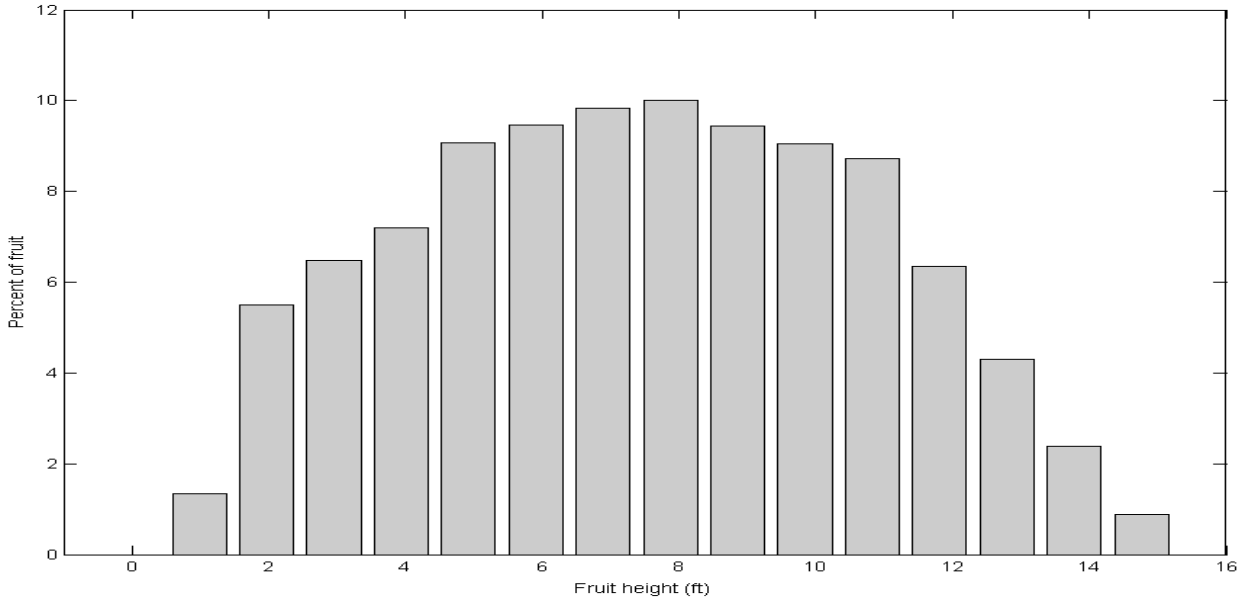

Fig. 22 Fruit height normalized histogram.

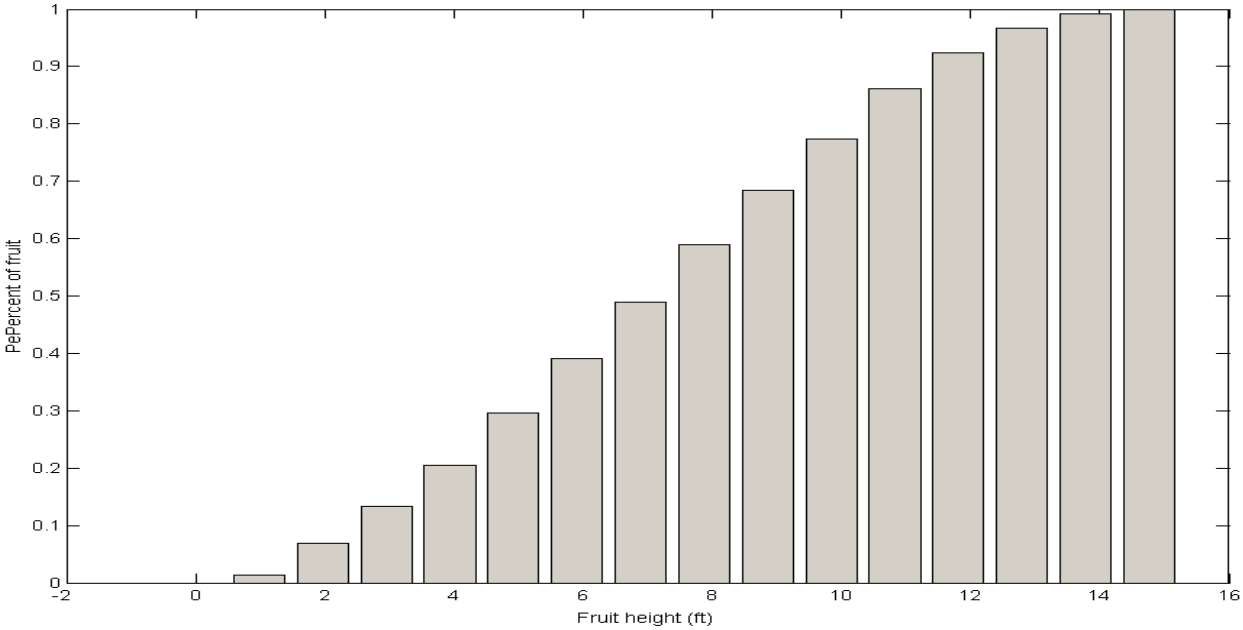

Fig. 23 Cumulative fruit height histogram.

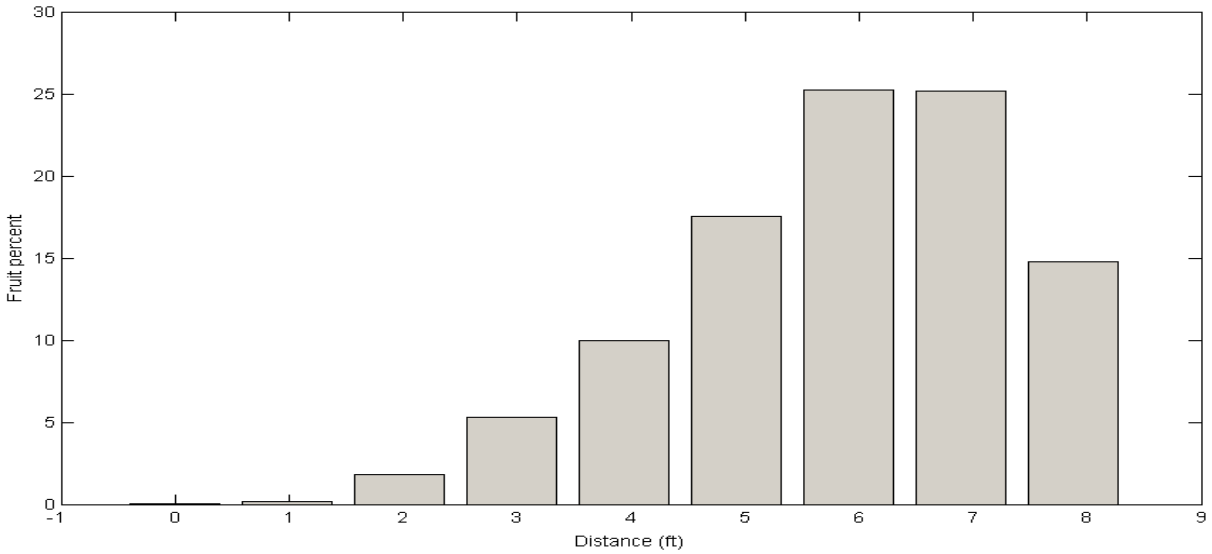

Fig. 24 Normalized histogram of fruit horizontal minimum distance from the left and right row centers.

The mean is E(d) = 5.83 ft, and σ = 1.44 ft, which is somewhat smaller than the pear trees measured at Ruddick Ranch.

4. DISCUSSION

The performance of the range measurement system was satisfactory and the accuracy achieved varied from 1'' to 8'', depending on the amount of foliage and line-of-sight conditions. However, in some instances the pickers would either pick fruit too quickly, or their bodies or the metallic ladders would interfere with the signal propagation path; this resulted in outliers in the data, i.e., ranges that were obviously erroneous or precision that was unacceptable (> 4''). These outliers were removed during the post-processing phase and the corresponding fruit positions were not included in the results. Experiments will be performed next summer and software tools have already been developed to detect such situations in real-time, so that they can be avoided.
Overall, fruit positions for more than 15,000 fruits were collected; such a large dataset has never been available in the past. The collected data will be used as input to rapid-prototyping software that will be developed to assist in the design and evaluation of orchard automation machinery. Some of these results have already been presented on November 28th at the workshop of the "Comprehensive Automation for Specialty Crops – CASC" SCRI project at Carnegie Mellon University and the responses of the researchers and farm advisors have been extremely positive. More dissemination activities have been scheduled for 2013.

ACKNOWLEDGEMENTS

We would like to thank Steve Johnson of Johnson Family Ranch, Chris Frieders of Joe Green Ranch, Jeff and Malcolm McCormack of Rivermaid Ranch, and Chris Ruddick of Ruddick Ranch for letting us gather data during their harvesting season. Finally, the

contributions of students Jason Wong and Farangis Khosro Anjom during the experiments, and Raj Rajkishan during data processing are greatly appreciated.